J Radioanal Nucl Chem (2016) 308:825–833
DOI 10.1007/s10967-015-4515-5

Radiocomplexation and evaluation of the ^{99m}Tc-Gemifloxacin in artificially *Escherichia coli* infected mice

M. Erfani[1] · M. Rekabgardan[2] · P. Mortazavi[2] · M. Shafiei[1]

Received: 24 June 2015 / Published online: 15 October 2015

Abstract Gemifloxacin as a broad spectrum quinolone antibacterial agent was radiocomplexed with high activity of ^{99m}Tc and was evaluated as an infection imaging agent in artificially *Escherichia coli* (*E. Coli*) infected mice. ^{99m}Tc-Gemifloxacin with high specific activity (0.148 GBq/μmol) and labeling yield (98.60 ± 0.70 %) was obtained. Our main achievement was high accumulation in the *E. Coli* infected right thigh muscle in mice (T/NT = 1.89 at 4 h post injection) which may diagnostically be beneficial to distinguish sites of *E. Coli* infection.

Keywords Direct labeling · Gemifloxacin · ^{99m}Tc · *Escherichia coli* · Infection imaging

Introduction

Currently, infection diseases are cause of many mortality in the world. Those bacteria that can cause infections are including *Streptococcus*, *Staphylococcus* and *E. coli* [1–3]. *Streptococcus* is a Gram-positive bacteria and responsible for many cases of disease like meningitis, bacterial pneumonia and endocarditis. *Staphylococcus* is a genus of Gram-positive bacteria can also cause a wide variety of diseases in humans and animals through either toxin production or penetration. *E. coli* is a gram-negative, rod-shaped bacterium and the virulent strains of which can cause various diseases such as gastroenteritis, urinary tract infections, and neonatal meningitis and in some rare cases, haemolytic-uremic syndrome, peritonitis, mastitis, septicemia and gram-negative pneumonia in human [4]. Intestinal mucosa-associated *E. coli* are observed in increased numbers in the inflammatory bowel diseases, Crohn's disease and ulcerative colitis [5]. Invasive strains of *E. coli* exist in high numbers in the inflamed tissue, and the number of bacteria in the inflamed regions correlates to the severity of the bowel inflammation [6]. *E. coli* is one of the varieties of bacterial species that have been reported to play a major role in acute appendicitis which is one of the most frequent conditions that leads to emergency abdominal surgery [7–9].

Nuclear imaging techniques as non-invasive diagnostic procedures in infection diseases can be used prior to invasive methods. Early detection is the other advantage of these techniques especially in cases like appendicitis, even in the beginning of infectious process that delay can lead to perforation, abdominal abscess, peritonitis, sepsis, and even death [10].

Several radiopharmaceuticals such as ^{111}In- or ^{99m}Tc-labeled white blood cells, ^{67}Ga-citrate and ^{111}In- or ^{99m}Tc labelled antibodies or antibody fragments, chemotactic peptides, liposomes and certain cytokines are used for SPECT imaging of infection and inflammation [11–15]. However, although these agents are widely accepted, none is considered satisfactory. In this way the research is now more focused on the development of particular tracers with more accuracy, sensitivity and specificity profile for the investigation of a particular infection or inflammation rather than searching for any ideal agent.

✉ M. Erfani
mgandomkar@aeoi.org.ir

[1] Radiation Application Research School, Nuclear Science and Technology Research Institute (NSTRI), North Kargar Ave, P.O. Box: 14395-836, Tehran, Iran

[2] Department of Basic Science, Faculty of Veterinary, Science and Research Branch, Islamic Azad University, P.O. Box: 14515-775, Tehran, Iran

Recently the ^{99m}Tc labeled cationic antimicrobial peptide derived from human ubiquicidine (UBI) has been proposed as an infection imaging agent [16, 17]. The results of the studies indicated that ^{99m}Tc-HYNIC-$UBI_{29–41}$ binds to bacteria and is accumulated at sites of infection [18–21]. As advancement in this field radiolabeled antibiotics have been developed which are highly specific for the microbial infections. [22, 23]. In different studies using labeled flouroquinolones, second and third generation cephalosporins, and also some antituberculous antibiotics their diagnostic specificity for the infection region have been showed [24–30]. However, antibiotics meet with the problem of antibiotic resistant bacteria [31, 32].

GMX [7-[(4*Z*)-3-(aminomethyl)-4-methoxyimino-pyrrolidin-1-yl]-1-yclopropyl-6-fluoro-4-oxo- 1,8-naphthyridine-3-carboxylic acid] is an oral broad spectrum quinolone antibacterial agent which has been shown to be active against most strains of the aerobic gram positive, aerobic gram negative and some other microorganisms [33]. It is used in the treatment of acute bacterial exacerbation of chronic bronchitis and mild-to-moderate pneumonia [34]. It acts by inhibiting DNA synthesis through the inhibition of both DNA gyrase and topoisomerase IV (TOPO IV), which are essential for bacterial growth [35]. Radiolabeling of GMX with ^{99m}Tc was performed by Shah et al. in 2011 for detecting *Streptococcus pneumoniae* infection with favorable results [36]. As early and rapid detection plays a vital role in the treatment outcome of some major diseases caused by *E. Coli*, in the present study our focus was on the development of a particular radiocomplex for imaging these infections. So, in order to achieve a radiocomplex with high accumulation in *E. Coli* infection, we hereby survey the optimized condition in preparation of ^{99m}Tc-GMX, stability in normal saline and human serum, lipophilicity, binding to *E. Coli* and its biological evaluation in artificially *E. Coli* infected mice as an in vivo scintigraphic agent.

Experimental

Materials and methods

Gemifloxacin mesylate obtained from Life Sciences Pharmaceuticals (LSP). All other chemicals obtained from Sigma-Aldrich and were used without further purification. Pertechnetate ($^{99m}TcO_4^-$) was eluted from the alumina based an in-house ^{99}Mo/^{99m}Tc generator with saline solution (0.9 % NaCl), and its activity was determined in a dose calibrator (Isomed, Germany). Quantitative gamma counting was performed using an EG&G/ORTEC Model 4001 M Mini Bin & Power Supply NaI(Tl) counter.

Preparation of ^{99m}Tc-GMX

A stock solution of GMX (concentration 20 mg/mL) was prepared by dissolving GMX in double distilled water. From this stock solution different amounts of GMX (0.5–5 mg) were carefully transferred to a vial. To this solution 20–100 μL (2 mg/mL) of freshly prepared stannous chloride dihydrate ($SnCl_2{\cdot}2H_2O$) in nitrogen purged 0.1 M HCl was added into vial. Effect of different amounts of stannous chloride and also change of pH factor in formation were investigated. Radiolabeling of the formulation involves initial warming up of the vial to room temperature followed by the addition of 740 MBq of freshly eluted $^{99m}TcO_4^-$ in maximum 1 mL of normal saline and incubation of the vial for 15 min at room temperature.

^{99m}Tc-GMX analysis

The ^{99m}Tc-GMX was characterized in NaCl 0.9 % (W/V) and in terms of radiochemical purity using thin layer radiochromatography (TLRC) and high performance liquid radiochromatography (HPLRC) system. TLRC plates (silica gel) were developed in ethanol:water:ammonium hydroxide (2:5:1 v/v) as well as in acetone. In the first solvent, free $^{99m}TcO_4^-$ and ^{99m}Tc-GMX move with solvent front with $R_f = 1$ and the reduced technetium remain at the point of application ($R_f = 0$). In the second solvent, $^{99m}TcO_4^-$ move with solvent front with $R_f = 1$ and the other species remain at the point of application. The radioactivity was quantified by cutting the strip (1.5×10 cm^2) into 1 cm pieces and counting in a well type gamma counter.

For radiochemical analysis by HPLRC 20 μL aliquots were taken out at 1, 4 and 6 h post reconstitution at room temperature and injected into the system with a JASCO 880-PU intelligent pump (Tokyo, Japan) equipped with a multiwavelength detector and a flow-through Raytest-Gabi γ-detector. CC 250/4.6 Nucleosil 120-5 C-18 column from Teknokroma was used. 0.1 % trifluoroacetic acid/water (Solvent A) and 0.1 % trifluoroacetic acid/acetonitrile (Solvent B) were used as a mobile phase in the following gradient: 0 min 95 % A (5 % B), 5 min 95 % A (5 % B), 25 min 0 % A (100 % B), 30 min 0 % A (100 % B), flow = 1 mL/min, $\lambda = 280$ nm.

Serum stability

Serum stability and radiocomplex transferred to serum protein was studied using the reported method [37]. Briefly, 1 mL of freshly prepared human serum was added to 100 μL of ^{99m}Tc-GMX. The mixture was incubated in 37 °C for 6 h. During incubation, samples of 100 μL aliquots were removed from the mixture after 1, 2, 4 and 6 h

and treated with 100 μL of absolute ethanol. After that, the samples were centrifuged at 3000 rpm in 4 °C for 5 min to precipitate serum proteins. Radiochemical stability in serum was determined by taking samples of 20 μL of supernatant at different times up to 6 h incubation that were analyzed by HPLRC.

Lipophilicity determination

0.5 mL of the ^{99m}Tc-GMX was mixed with 0.5 mL of octanol in a 2 mL micro tube. The tube was vigorously vortexed over a period of 10 min and centrifuged at 3000×*g* for 5 min. Three aliquots of 100 μl were sampled from each layer and counted in the γ counter. The averaged activities from the aqueous and the octanol layers were used to calculate the log *P* values. The octanol-to-water partition coefficient ($P_{o/w}$) was calculated by dividing the counts of the octanol phase by that of the aqueous phase.

In vitro binding with *Escherichia coli*

100 μL of the ^{99m}Tc-GMX was transferred to a test tube. Then, 0.9 mL of 50 % (v/v) 0.01 M acetic acid in phosphate buffer (pH 7.5) containing approximately 1×10^8 colony forming units (CFU) per mL viable *E. Coli* was added. The mixture was incubated for 1 h at 4 °C and thereafter the vials were centrifuged in a pre-cooled centrifuge at 2000×*g* at 4 °C for 5 min. The supernatant was removed, and analyzed by HPLRC method for evaluation of stability of ^{99m}Tc-GMX in incubated medium and binding condition. The bacterial pellet was gently re-suspended in 1 mL of buffer and re-centrifuged as above. The supernatant was again removed leaving the bacterial pellets in the test tube, which were counted for percent uptake by a gamma counter.

Biodistribution in *E. Coli* infected mice model

Animal experiments were performed in compliance with the regulations of our institution and with generally accepted guidelines governing such work (No 642). Male Balb/c mice (25–30 g) were infected by injection 0.1 mL of saline containing 1×10^8 colony-forming unit (CFU) *E. Coli* bacteria into right thigh muscle through needle gauge 19. Mice also were inflamed by injection of 0.1 mL of autoclaved turpentine oil into right thigh muscle. After 24 h, a group of three balb/c mice (25–30 g, 6 week) received 0.37 MBq of ^{99m}Tc-GMX in volume of 0.1 mL via a tail vein. The mice were sacrificed at different post injection times (1, 4 and 6 h) and the tissues and organs of interest were collected, immediately weighed and counted in a NaI well-type γ-counter. Subsequently, percentage uptake of the ^{99m}Tc-GMX in one gram of the blood, heart, lung, stomach, intestine, thyroid, liver, spleen, kidney, infected muscle (T) and normal muscle (NT) of balb/c mice was calculated as the percentage of the injected dose per gram tissue (%ID/g tissue). The values are expressed as mean ± SD.

Imaging studies

At time points of 1 and 4 h after injection, accumulation of the ^{99m}Tc-GMX in infected area was assessed by planar scintigraphy using the single head gamma camera (small area mobile, Siemens, 140 keV high sensitivity parallel whole collimator and 10 % window around 140 keV). Before the imaging, mice were anesthetized with 0.05 mL ketamine 10 % (3.3 mg) and 0.05 mL xylazine 2 % (1.33 mg) intra-peritoneally. After about 5 min, the animal was fixed on a board by covering with pieces of cloth for immobilization during the scanning.

Results and discussion

Radiocomplexation

The ^{99m}Tc-GMX structure as shown in Fig. 1 was prepared by reducing ^{99m}Tc in $^{99m}TcO_4^-$ with stannous chloride. Technetium can have a number of oxidation states but the +5 oxidation state is the most common in Tc = O complexes, with d^2 configuration. Crystal structural studies have shown that when the atoms implicated in coordination are π-donor Lewis bases as in the present case then the square pyramidal structure is very favored [38, 39]. Based on the above description, this Tc^{+5} = O ^{99m}Tc-GMX will have a square pyramidal configuration having ^{99m}Tc to ligand ratio of 1:2.

In order to identify an easy to use synthetic route with a high radiolabeling yield of ^{99m}Tc-GMX, radiolabeling was performed by varying reaction parameters such as the amount of ligand, amount of reducing agent and the pH value of reaction system.

Highly radioactive ligands can suffer radiation damage and the presence of radioactive impurities will almost certainly lead to a reduction of the ratio of specific to non specific labeling therefore reducing the amount of ligand used in the formulation is still highly desirable. Also increasing the amount of ligand, the issue of solubility's is raised. Our observation shows that if we increase the ligand concentration, solubility's decrease. Therefore, one of the objectives was to reduce the amount of ligand used in the labeling process. As Table 1 shows 2 mg of ligand was the optimum amount of ligand in formulation to reach a high labeling yield for formation ^{99m}Tc-GMX.

Fig. 1 Proposed structure of the ^{99m}Tc-GMX

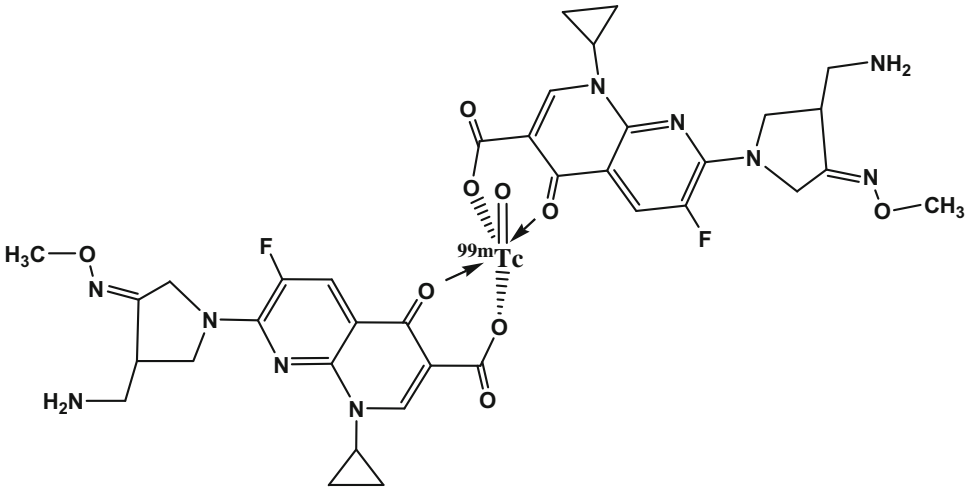

Table 1 Influence of different amount of ligand on preparation yield of ^{99m}Tc-GMX

Amount of ligand (mg)	Preparation yield (%)
0.5	61.2 ± 3.5
1.0	81.4 ± 4.3
1.5	92.6 ± 3.5
2.0	98.6 ± 0.7
2.5	96.7 ± 1.2
5.0	94.5 ± 1.8

Values are expressed as mean ± SD ($n = 3$)

$SnCl_2{\cdot}2H_2O$ was used to reduce ^{99m}Tc in $^{99m}TcO_4^-$ (VII) to its lower oxidation state (V) and enable ^{99m}Tc (V) to react with the ligand. The best amounts of $SnCl_2{\cdot}2H_2O$ is required were observed to be 80–120 μg. As has been shown in Fig. 2 employing concentration of reducing agent less than 80 μg will not reduce all of $^{99m}TcO_4^-$(VII) to its lower oxidation state ^{99m}Tc (V) which in turn cause to lower labeling yield. On the other hand choosing concentration more than 120 μg further reduction of ^{99m}Tc (VII) to its lower oxidation state ^{99m}Tc (IV) is possible in which a colloidal $^{99m}TcO_2$ is formed in aqueous media and as a result labeling yield also was reduced. It can be concluded that a stable ^{99m}Tc-GMX with high radiochemical purity (98.60 ± 0.70 %) can be acquired with use of 100 μg $SnCl_2{\cdot}2H_2O$ (Fig. 2).

The effect of reaction pH was also investigated and the optimal pH range to produce a high labeling yield was found to be between pH 4–5 (Fig. 3). The yield decrease as pH varies from above range. As a coordination complex of ^{99m}Tc is formed by means of bonds between technetium acting as Lewis acid and functional groups which act as Lewis bases (donate electron pairs), in the basic medium carboxylic moiety of GMX is neutralized and is not able to produce a stable complex with ^{99m}Tc.

^{99m}Tc-GMX was prepared in optimized condition (2 mg/100 μL GMX, 100 μg/50 μL $SnCl_2{\cdot}2H_2O$ in 0.1 M

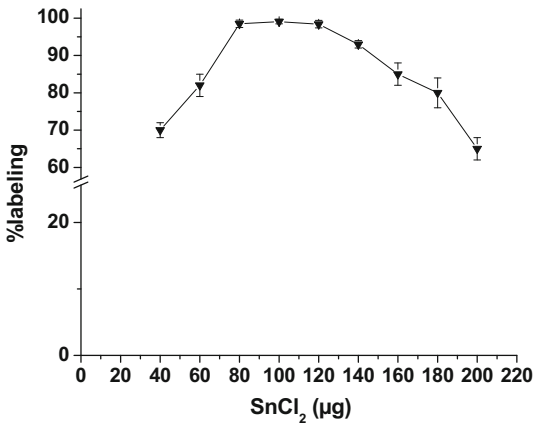

Fig. 2 Effect of $SnCl_2{\cdot}2H_2O$ on preparation yield of ^{99m}Tc-GMX. Values are expressed as mean ± SD ($n = 3$)

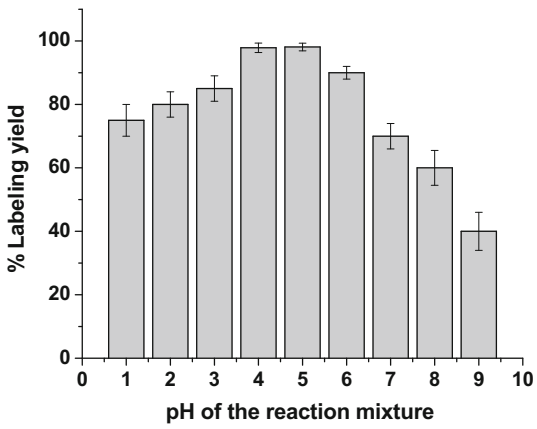

Fig. 3 Effect of reaction pH on ^{99m}Tc-GMX labeling yield. Values are expressed as mean ± SD ($n = 3$)

HCl, 370 MBq/1 mL of $^{99m}TcO_4^-$, pH 4–5) for 15 min at room temperature (specific activity of 64.3 MBq/nmol). In the formulation reported previously [36], in best condition 2 mg of GMX has been labeled with 111 MBq of $^{99m}TcO_4^-$ which is more than tree time lower in specific activity compared with our product. They used 125 μg $SnCl_2{\cdot}2H_2O$ as a reducing agent and final pH for their formulation was 5.4. The higher specific activity obtained in our radiocomplexation could be duo to our optimized condition.

Radiochemical purity

The radiochemical purity of ^{99m}Tc-GMX was determined by TLRC. In the first part a solvent system which consisted of ethanol: water: ammonium hydroxide (2:5:1 v/v) employed as a mobile phase. The activity remained in the origin was negligible and corresponding to reduced ^{99m}Tc (Fig. 4a). In the second part choosing acetone as a solvent, the ^{99m}Tc-GMX remain at the origin (Rf = 0) where as free ^{99m}Tc pertechnetate will migrate with solvent front (Rf = 1) and its activity was near the background (Fig. 4b). ^{99m}Tc-GMX showed 98.60 ± 0.70 % radiochemical yield at specific activity of 0.148 GBq/μmol. In characterization of ^{99m}Tc-GMX by HPLRC two different peaks with retention times of 4.51 min and 14.55 min were observed (Fig. 5). The ^{99m}Tc complex has been characterized by comparison with the corresponding ligand. The UV-HPLRC chromatogram retention time of ligand was observed to be 15.25 min, which matches well with 14.55 min γ-HPLRC chromatogram retention time of ^{99m}Tc-GMX.

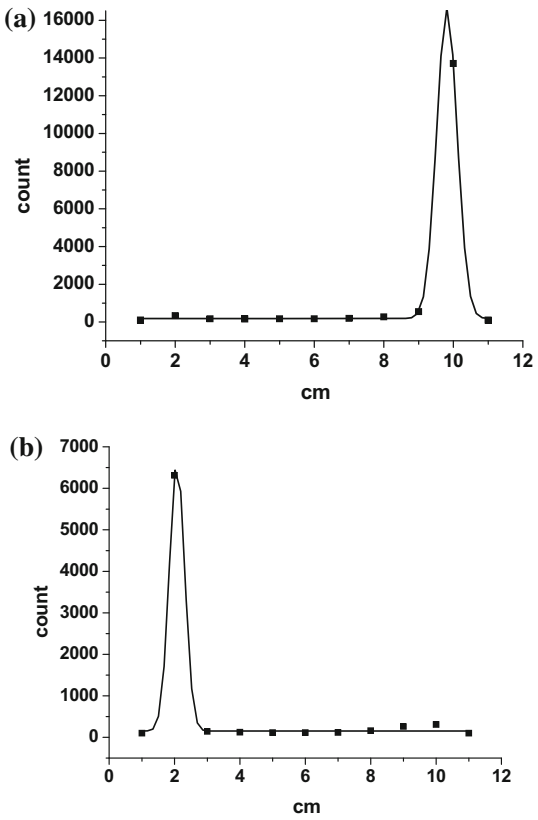

Fig. 4 TLRC chromatograms of ^{99m}Tc-GMX developed in ethanol:water:ammonium hydroxide (2:5:1 v/v) with ^{99m}Tc-GMX in $R_f = 1$ and $^{99m}TcO_2$ in $R_f = 0$ (**a**) and in acetone solvent with ^{99m}Tc-GMX in $R_f = 0$ and $^{99m}TcO_4$ in $R_f = 1$ (**b**). ^{99m}Tc-GMX showed 98.60 ± 0.70 % labeling yield

Stability and binding to *E. Coli*

The radiochemical purity of the ^{99m}Tc-GMX was >95 % over the observed period of 6 h (Fig. 6). No decomposition of the complex was observed in this time period, suggesting its high stability in normal saline at room temperature. Radiochemical stability of ^{99m}Tc-GMX in human serum was >90 % up to 6 h indicating its quality of being appropriate from stability outlook (Fig. 6). So far the main drawback in labeling of ciprofloxacin and its similar structures are colloid impurity and their instability which were subject of discussion in previous studies by different groups [40, 41] but here with optimization of labeling condition high labeling yield and stability for ^{99m}Tc-GMX is achieved.

The radiocomplex transferred to human serum proteins was about 66 ± 7 % after 6 h. The partition coefficient of the ^{99m}Tc-GMX was determined by distribution in octanol and water, and its log P value was found to be −0.12 ± 0.04, signifying low lipophilicity which could

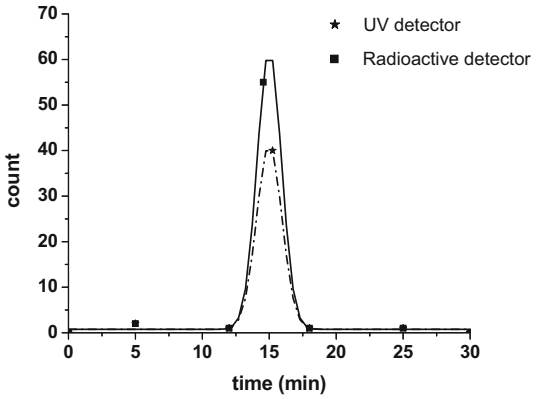

Fig. 5 Reversed phase HPLRC chromatogram for ligand in multi-wavelength detector (λ = 280 nm) (**a**) and for ^{99m}Tc-GMX in Raytest-Gabi γ-detector (**b**). CC 250/4.6 Nucleosil 120-5 C-18 column from Teknokroma was used. 0.1 % trifluoroacetic acid/water (Solvent A) and 0.1 % trifluoroacetic acid/acetonitrile (Solvent B) were used as a mobile phase in the following gradient: 0 min 95 % A (5 % B), 5 min 95 % A (5 % B), 25 min 0 % A (100 % B), 30 min 0 % A (100 % B), flow = 1 mL/min

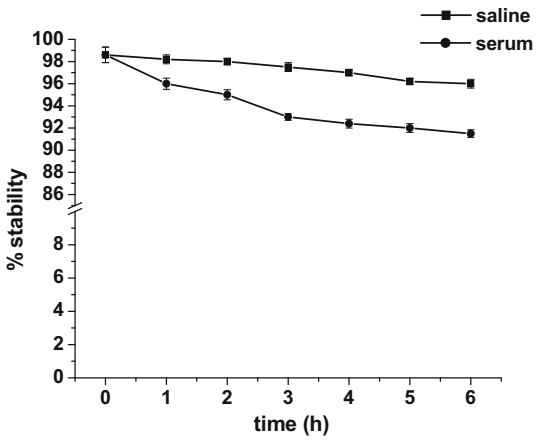

Fig. 6 In vitro stability of the ^{99m}Tc-GMX at different time in saline and serum

explain the accumulation of the ^{99m}Tc-GMX in the kidney and liver. *In vitro* binding of ^{99m}Tc-GMX to *E. Coli* is shown in Fig. 7. The ^{99m}Tc-GMX radioactivity bound to bacteria was 34.6 % at 1 h after incubation while this value was significantly low for $^{99m}TcO_4^-$ (9.0 %) which showed the binding was specific. No decomposition of ^{99m}Tc-GMX was observed in HPLRC which is also an indication of the stability of ^{99m}Tc-GMX in the evaluated condition.

Biodistribution and imaging

Biological evaluation of ^{99m}Tc-GMX was performed in Balb/c mice. The results are shown in Tables 2, 3 and Fig. 8. The uptake value for blood was high and with mild clearance decreased from 8.42 ± 1.50 %ID/g at 1 h to 2.56 ± 1.55 %ID/g at 4 h. Similarly, the level of the ^{99m}Tc-GMX in liver decreased from 18.48 ± 2.45 %ID/g at 1 h to 17.73 ± 2.27 %ID/g at 4 h post injection. For the kidneys the ^{99m}Tc-GMX showed decreasing uptake from 14.26 ± 1.35 %ID/g at 1 h to 11.84 ± 1.51 %ID/g at 4 h

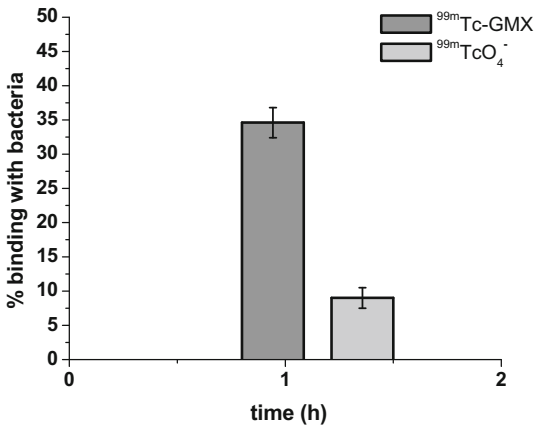

Fig. 7 In vitro binding of ^{99m}Tc-GMX with *E. Coli* in comparison with $^{99m}TcO_4^-$ 1 h after incubation at 4 °C

post injection. The presence of the high activity in liver and kidney suggesting that the hepatobiliary and urinary systems is the major route of excretion of administered radioactivity.

The radioactivity concentration of infected muscle by *E. Coli* at 1 h post injection was 1.64 ± 0.15 %ID/g which decreased to 1.27 ± 0.12 %ID/g at 4 h post injection. The ratio uptake of T/NT was 1.49 at 1 h post injection and 1.89 at 4 h post injection also ratio for infected muscle to inflamed muscle was 1.43 and 1.89 at 1 and 4 h post injection respectively. The increase of the T/NT ratio as time elapsed from 1 to 4 h is may be due to the clearance of non specific uptake from normal and inflamed regions and on the other hand this high value for retention shows ^{99m}Tc-GMX have specific affinity to Gram-negative bacterial infection site, although the radioactivity concentration in infectious muscle at 4 h post injection is lower than 1 h post injection. The uptake of ^{99m}Tc-GMX in inflamed muscle was similar to normal muscle which showed that its uptake was not specific in aseptic inflammation regions and confirmed the affinity of ^{99m}Tc-GMX for infected muscles due to its specific binding.

In previous study Streptococcus pneumonia infected rats was used to assess the in vivo behavior of the ^{99m}Tc-Gemifloxacin [36]. The ratio of T/NT activity which accumulated at the site of infectious muscle compared to normal muscle was 3.25 in the Streptococcus pneumonia model. In the present study although ^{99m}Tc-GMX was prepared with high specific activity, accumulation of ^{99m}Tc-GMX was lower in the *E. Coli* induced infection model compared to the Streptococcus pneumonia model which show lower susceptibility of ^{99m}Tc-GMX for *E. Coli* induced abscess. In another study by Sah et al. [26] ^{99m}Tc-fleroxacin has been evaluated for *E. Coli* infection imaging. Their results showed uptake ratio of 2.78 for infected to inflamed muscle at 1 h post injection while the blood and stomach-intestines uptake were 11.2 ± 1.50 and 7.25 ± 1.50 %ID/g at 1 h post injection respectively. Compared to our results although the ratio for infected to inflamed muscle ^{99m}Tc-fleroxacin was higher than that of ^{99m}Tc-GMX (2.78 vs 1.49) however values for blood, stomach and intestines for ^{99m}Tc-GMX was lower than that of for ^{99m}Tc-fleroxacin (8.42 ± 1.50, 1.68 ± 1.00 (means uptake values for stomach and intestines) %ID/g at 1 h versus 11.2 ± 1.50 and 7.25 ± 1.50 %ID/g at 1 h post injection respectively). This high uptake for ^{99m}Tc-fleroxacin especially in stomach and intestine is an indication of the in vivo instability of the radiocomplex which subsequently could prevent accurate diagnosis of *E. Coli* infection in the intestine, especially in the case of intestinal infections such as appendicitis. On the other hand ^{99m}Tc-GMX low stomach and intestine activity uptake would be an advantage for imaging of abdominal infection diseases.

Table 2 Biodistribution of ^{99m}Tc-GMX in artificially *E. Coli* infected mice (%ID/g ± SD, $n = 3$)

Organs	Post-injection time (h)		
	1	4	6
Blood	8.42 ± 1.50	2.56 ± 1.55	1.94 ± 0.64
Heart	3.41 ± 1.15	1.41 ± 0.94	1.37 ± 0.64
Lung	4.96 ± 1.21	2.54 ± 0.96	1.75 ± 0.56
Stomach	1.26 ± 0.54	0.63 ± 0.25	1.15 ± 0.42
Intestine	2.11 ± 1.46	2.20 ± 0.98	1.54 ± 0.45
Thyroid	2.23 ± 1.22	1.44 ± 0.76	1.34 ± 0.69
Liver	18.48 ± 2.45	17.73 ± 2.27	12.45 ± 1.87
Spleen	5.63 ± 0.97	4.64 ± 0.87	2.75 ± 0.53
Kidney	14.26 ± 1.35	11.84 ± 1.51	8.61 ± 1.43
Normal muscle	1.10 ± 0.14	0.67 ± 0.13	0.52 ± 0.07
E. Coli infected muscle	1.64 ± 0.15	1.27 ± 0.12	0.82 ± 0.08

Table 3 Biodistribution of ^{99m}Tc-GMX in aseptic inflamed mice (%ID/g ± SD, $n = 3$)

Organs	Post-injection time (h)		
	1	4	6
Blood	8.16 ± 1.50	2.36 ± 1.24	1.45 ± 0.19
Heart	3.25 ± 1.34	1.31 ± 0.74	0.92 ± 0.13
Lung	4.45 ± 1.21	2.75 ± 0.75	1.69 ± 0.35
Stomach	2.15 ± 0.57	1.25 ± 0.41	1.56 ± 0.31
Intestine	2.62 ± 1.46	2.10 ± 0.61	1.41 ± 0.31
Thyroid	2.10 ± 1.12	1.25 ± 0.28	1.21 ± 0.19
Liver	17.31 ± 1.29	16.21 ± 1.75	11.31 ± 0.82
Spleen	5.65 ± 0.29	4.65 ± 0.30	2.12 ± 0.32
Kidney	14.10 ± 0.51	11.46 ± 1.12	8.41 ± 0.64
Aseptic inflamed muscle	1.15 ± 0.12	0.70 ± 0.11	0.54 ± 0.09

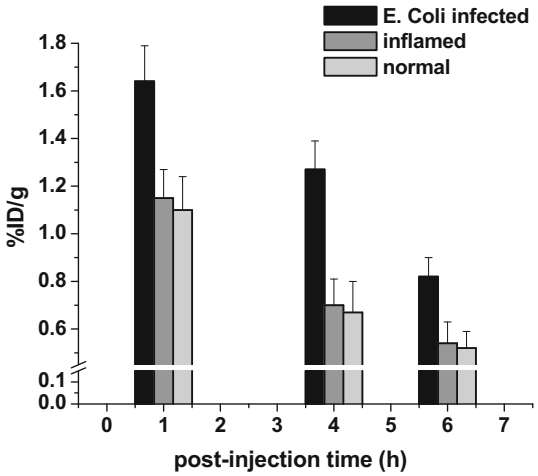

Fig. 8 The comparison uptake of ^{99m}Tc-GMX in *E. Coli* infected muscles with normal and inflamed muscles of mice at different time point (1, 4 and 6 h) after injection

An imaging study at 4 h post injection showed uptake for ^{99m}Tc-GMX in the site of infection (Fig. 9). The uptake in all organs was decreased significantly after 6 h which shows that elimination is time depended and the early time up to 4 h is the best time for infection detection.

Conclusion

Gemifloxacin belongs to the class of medicines known as quinolone antibiotics. It works by killing bacteria or preventing their growth. Gemifloxacin is used to treat bronchitis and pneumonia caused by bacterial infections. Since Gemifloxacin is active against bacteria such as *E. Coli* it is expected that ^{99m}Tc-GMX can play a role in diagnose of infection diseases with *E. Coli* origin. In this study, we have shown preparation and evaluation of a ^{99m}Tc-GMX with high labeling yield. Based on the data obtained from this study, the ^{99m}Tc-GMX was stable, reproducible with high labeling efficiency with desirable characteristics making it a promising agent for imaging of Gram-negative infectious lesions. According to the results of in vivo biodistribution studies, we found that the uptake by infectious sites is high and has a good retention time. These

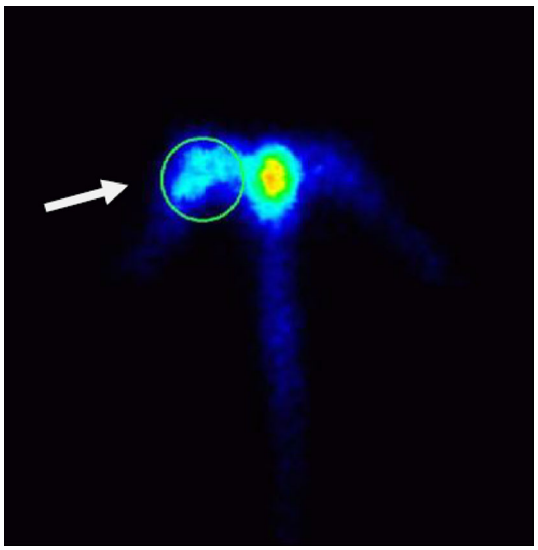

Fig. 9 Anterior scintigraphy of mice with right thigh muscle artificially *E. Coli* infected 4 h post injection of ^{99m}Tc-GMX after masking of abdominal region while infection site has been shown with *arrow*

promising characteristics make ^{99m}Tc-GMX as a very suitable candidate for diagnostic of *E. Coli* infectious sites in nuclear medicine. Further investigation on the ability of ^{99m}Tc-GMX to bind and detect other bacteria strains should be pursued.

Acknowledgments The authors would like to thank Mr. Mazidi and Mr Talebi for their excellent technical assistance in experiments and biodistribution studies.

References

1. Edwards MS, Baker CJ (2005) Group B streptococcal infections in elderly adults. Clin Infect Dis 41(6):839–847
2. Fowler VG, Olsen MK, Corey GR, Woods CW, Cabell CH, Reller LB, Cheng AC, Dudley T, Oddone EZ (2003) Clinical identifiers of complicated *Staphylococcus aureus* bacteremia. Arch Intern Med 163(17):2066–2072
3. Su C, Brandt LJ (1995) *Escherichia coli* O157:H7 infection in humans. Ann Intern Med 123:698–714
4. Pathogenic E. coli, Online textbook of bacteriology. University of Wisconsin-Madison Department of Bacteriology. http://textbookofbacteriology.net/e.coli.html. Retrieved 30 Nov 2007
5. Rolhion N, Darfeuille-Michaud A (2007) Adherent-invasive *Escherichia coli* in inflammatory bowel disease. Inflamm Bowel Dis 13(10):1277–1283
6. Baumgart M, Dogan B, Rishniw M, Weitzman G, Bosworth B, Yantiss R, Orsi RH, Wiedmann M, McDonough P, Kim SG, Berg D, Schukken Y, Scherl E, Simpson KW (2007) Culture independent analysis of ileal mucosa reveals a selective increase in invasive *Escherichia coli* of novel phylogeny relative to depletion of Clostridiales in Crohn's disease involving the ileum. ISME J 1(5):403–418
7. Chen CY, Chen YC, Pu HN, Tsai CH, Chen WT, Lin CH (2012) Bacteriology of acute appendicitis and its implication for the use of prophylactic antibiotics. Surg Infect (Larchmt) 13(6):383–390
8. Bennion RS, Baron EJ, Thompson JE Jr, Downes J, Summanen P, Talan DA, Finegold SM (1990) The bacteriology of gangrenous and perforated appendicitis-revisited. Ann Surg 211:165–171
9. Lau WY, Teoh-Chan CH, Fan ST, Yam WC, Lau KF, Wong SH (1984) The bacteriology and septic complication of patients with appendicitis. Ann Surg 200:576–581
10. Rypins EB, Evans DG, Hinrichs W, Kipper SL (1997) Tc-99m-HMPAO white blood cell scan for diagnosis of acute appendicitis in patients with equivocal clinical presentation. Ann Surg 226(1):58–65
11. Sfakianakis GN, Al-Sheith W, Heal A, Rodman G, Zeppa R, Serafini A (1982) Comparisons of scintigraphy with In-111 leucocyte and Ga-67 in the diagnosis of occult sepsis. J Nucl Med 23:618–626
12. Peters AM (1994) The utility of Tc-99m-HMPAO leucocytes for imaging infection. Semin Nucl Med 24:110–127
13. Harvey J, Cohen MM (1997) Technetium-99-labeled leukocytes in diagnosing diabetic osteomyelitis in the foot. J Foot Ankle Surg 36:209–214
14. Rypins EB, Kipper SL (2000) Scintigraphic determination of equivocal appendicitis. Am Surg 66(9):891–895
15. Rennen HJ, Oyen WJ, Cain SA, Monk PN, Corstens FH, Boerman OC (2003) Tc-99m-labeled C5a and C5a des Arg74 for infection imaging. Nucl Med Biol 30:267–272
16. Akhtar MS, Qaisar A, Irfanullah J, Iqbal J, Khan B, Jehangir M, Nadeem MA, Khan MA, Afzal MS, Ul-Haq I, Imran MB (2005) Antimicrobial peptide ^{99m}Tc-ubiquicidin 29-41 as human infection-imaging agent: clinical trial. J Nucl Med 46(4):567–573
17. Gandomkar M, Najafi R, Mazidi M, Goudarzi M, Mirfallah SH (2008) New peptide based freeze-dried kit [^{99m}Tc-HYNIC]-UBI 29-41 as a human specific infection imaging agent. Iran J Nucl Med 16(1):25–30
18. Sepúlveda-Méndez J, de Murphy CA, Rojas-Bautista JC, Pedraza-López M (2010) Specificity of ^{99m}Tc-UBI for detecting infection foci in patients with fever in study. Nucl Med Commun 31(10):889–895
19. Gandomkar M, Najafi R, Shafiei M, Mazidi M, Goudarzi M, Mirfallah SH, Ebrahimi F, Heydarpor HR, Abdie N (2009) Clinical evaluation of antimicrobial peptide [^{99m}Tc/Tricine/HYNIC^0]ubiquicidin 29-41 as a human-specific infection imaging agent. Nucl Med Biol 36(2):199–205
20. Assadi M, Vahdat K, Nabipour I, Sehhat MR, Hadavand F, Javadi H, Tavakoli A, Saberifard J, Kalantarhormozi MR, Zakani A, Eftekhari M (2011) Diagnostic value of ^{99m}Tc-ubiquicidin scintigraphy for osteomyelitis and comparisons with ^{99m}Tc-methylene diphosphonate scintigraphy and magnetic resonance imaging. Nucl Med Commun 32(8):716–723
21. Beikia D, Yousefia G, Fallahia B, Tahmasebib MN, Gholamrezanezhada A, Fard-Esfahania A, Erfani M, Eftekhari M (2013) ^{99m}Tc-Ubiquicidin [29–41], a promising radiopharmaceutical to differentiate orthopedic implant infections from sterile inflammation. Iran J Pharm Res 12(2):347–353
22. Benitez A, Roca M, Martin-comin J (2006) Labeling of antibiotics for infection diagnosis. Q J Nucl Med Mol Imaging 50:147–152
23. Lambrecht FY (2011) Evaloation of ^{99m}Tc-labeled antibiotics for infection detection. Ann Nucl Med 25:1–6
24. Erfani M, Doroudi A, Hadisi L, Andishmand A, Mirshojaei SF, Shafiei M (2013) ^{99m}Tc-tricabonyl labeling of ofloxacin and its biological evaluation in Staphylococcus aureus as an infection imaging agent. J Label Compd Radiopharm 56:627–631
25. Roohi S, Mushtaq A, Jehangir M, Ashfaq MS (2006) Synthesis, quality control and biodistribution of ^{99m}Tc-Kanamycin. J Radioanal Nucl Chem 267:561–566
26. Shah SQ, Khan MR (2011) Radiosynthesis and characterization of the ^{99m}Tc-fleroxacin complex: a novel *Escherichia coli* infection imaging agent. Transit Met Chem 36:283–287

27. Shah SQ, Khan MR (2011) Synthesis of ^{99m}Tc V:N-Pazufloxacin dithiocarbamate complex and biological evaluation in Wistar rats artificially infected with *Escherichia coli*. J Radioanal Nucl Chem 288:511–516
28. Chattopadhyay S, Das S, Chandra S, De K, Mishra M, Sarkar B, Sinha S, Ganguly S (2010) Synthesis and evaluation of ^{99m}Tc-moxifloxacin a potential infection specific imaging agent. Appl Radiat Isot 68:314–316
29. Zhang J, Guo H, Zhang S, Lin Y, Wang X (2008) Synthesis and biodistribution of a novel ^{99m}TcN complex of ciprofloxacin dithiocarbamate as a potential agent for infection imaging. Bioorg Med Chem Lett 18:5168–5170
30. Motaleb M (2007) Preparation of ^{99m}Tc-cefoperazone complex, a novel agent for detecting sites of infection. J Radioanal Nucl Chem 272:167–171
31. Limoncu MH, Ermertcan S, Cetin CB, Cosar G, Dinc G (2003) Emergence of phenotypic resistance to ciprofloxacin and levofloxacin in methicillin-resistant and methicillin-sensitive *Staphylococcus aureus* strains. Int J Antimicrob Agents 5:420–424
32. Fewton KA, Ison C, Johnson AP, Rudd E, Soltani M, Martin I, Nichols T, Livermore DM (2003) Ciprofloxacin resistance in *Neisseria gonorrhoeae* in England and Wales in 2002. Lancet 361:1867–1869
33. Cormican MG, Jones RN (1997) Antimicrobial activity and spectrum of LB20304, a novel fluoronaphthyridone. Antimicrob Agents Chemother 41:204–211
34. Calvo A, Gimenez MJ (2002) Ex vivo serum activity (killing rates) after gemifloxacin 320 mg versus trovafloxacin 200 mg single doses against ciprofloxacin-susceptible and-resistant *Streptococcus pneumoniae*. Int J Antimicrob Agents 20(2):144–146
35. Fournier B, Zhao X, Lu T, Drlica K, Hooper DC (2000) Selective targeting of topoisomerase IV and DNA gyrase in *Staphylococcus aureus*: different patterns of quinolone-induced inhibition of DNA synthesis. Antimicrob Agents Chemother 44(8):2160–2165
36. Shah SQ, Khan MR (2011) Radiolabeling of gemifloxacin with technetium-99 m and biological evaluation in artificially *Streptococcus pneumoniae* infected rats. J Radioanal Nucl Chem 288:307–312
37. Zhang H, Chen J, Waldherr C, Hinni K, Waser B, Reubi JC, Maecke HR (2004) Synthesis and evaluation of bombesin derivatives on the basis of pan-bombesin peptides labeled with Indium-111, Lutetium-177, and Yttrium-90 for targeting bombesin receptor-expressing tumors. Cancer Res 64:6707–6715
38. Boschi A, Duatti A, Uccelli L (2005) Development of technetium-99 m and rhenium-188 radiopharmacueticals containing a terminal metal-nitrido multiple bond for diagnosis and therapy. Top Curr Chem 252:85–115
39. Bandoli G, Dolmella A, Porchia M, Tisato E, Refosco P (2001) Structural overview of technetium compounds (1993–1999). Coord Chem Rev 214:43–90
40. Motaleb MA (2007) Preparation and biodistribution of ^{99m}Tc-lomefloxacin and ^{99m}Tc-ofloxacin complexes. J Radioanal Nucl Chem 272:95–99
41. Bhardwaj N, Bhatnagar A, Singh AK (2005) Development and evaluation of a single vial cold kit for infection imaging: Tc-99m ciprofloxacin. World J Nucl Med 4:244–251